

# Comparing the influence of Floquet dynamics in various Kitaev-Heisenberg materials

Pascal Strobel<sup>1</sup> and Maria Daghofer<sup>1,2</sup>

<sup>1</sup>*Institut für Funktionelle Materie und Quantentechnologien, Universität Stuttgart, 70550 Stuttgart, Germany*

<sup>2</sup>*Center for Integrated Quantum Science and Technology,  
University of Stuttgart, Pfaffenwaldring 57, 70550 Stuttgart, Germany*

(Dated: November 1, 2021)

In this paper we examine the possibility of Floquet engineering in the three candidate Kitaev materials  $\text{Na}_2\text{IrO}_3$ ,  $\alpha\text{-Li}_2\text{IrO}_3$  and  $\alpha\text{-RuCl}_3$ . We derive an effective Floquet Hamiltonian and give an approximation for heating processes arising from doublon holon propagation. This suggests that compounds with stronger Hund's-rule coupling are less prone to heating. We then investigate the impact of light frequency and amplitude on magnetic interaction terms up to third-nearest-neighbor and find that third-neighbor Heisenberg coupling  $J_3$  is very susceptible to tuning by circularly polarized light. Finally, we discuss uses of linear polarized light in selectively tuning single bond directions.

## I. INTRODUCTION

Light-matter interactions with periodic driving have gathered significant attention recently [1–3]. In these systems the Floquet theorem is applicable, and they can be described with an effective time-independent Floquet Hamiltonian [4–7]. Frequency, amplitude, and polarization are then capable of changing intrinsic interactions of the system. This paves the way to tune magnetic properties of materials via the driving field. While for large time scales the system thermalizes, the Floquet Hamiltonian has been argued to be valid at short, but experimentally accessible, timescales [8].

Floquet engineering is especially promising for candidate Kitaev-Heisenberg materials [9]. Those materials are supposed to host a Kitaev spin liquid (KSL) for an idealized structure. However in reality most of them show a zig-zag ordering [10–13]. Tuning these materials from zig-zag to the KSL has been a focal point of theoretical and experimental research. While tuning via pressure [14–16], magnetic field [17–21], graphen substrates [22] and chemical doping [23–25] has been investigated extensively, the approach of driving the Kitaev phase via a periodic light field is yet relatively unexplored.

Driving with light periodic in time might allow to alter the relative strength of the interactions, and therefore give rise to a KSL. In particular, materials that are already proximate to the Kitaev phase should be a good starting point. Such materials are, e.g., iridates like  $\text{Na}_2\text{IrO}_3$  [26] and  $\alpha\text{-Li}_2\text{IrO}_3$  [27] and the ruthenate  $\alpha\text{-RuCl}_3$  [28]. Since these materials have already been studied in absence of a light field [12, 13, 27, 29, 30], we base our studies on already well-established models [26]. Previous studies on Floquet engineering [31] have focused on tuning nearest-neighbor interactions in  $\alpha\text{-RuCl}_3$  with circularly polarized light and highlighted the possibility of tuning Heisenberg interactions. However this phenomenon was just found after changing signs of a specific parameter. For iridates studies on Floquet engineering are still lacking.

In this paper we study the capabilities of Floquet

engineering, for  $\alpha\text{-RuCl}_3$  as well as for  $\alpha\text{-Li}_2\text{IrO}_3$  and  $\text{Na}_2\text{IrO}_3$ . First we consider an approximate approach to capture heating around the resonances [32] in order to identify frequencies where it is small. This gives an insight on which of these materials are well suited for Floquet engineering. Introducing linear polarized light instead of circular polarized light, interactions become bond dependent. This gives the possibility to tune the interactions via the light angle. We finally discuss third-nearest-neighbor Heisenberg coupling. It was found to be significant in ruthenates (and iridates) and is argued to be responsible for the zig-zag magnetic ordering [30].

The paper is structured as follows: In Sec. II we derive the effective Floquet Hamiltonian for the Kitaev-Heisenberg model, applying the results of [7, 32, 33] to the already well established Kitaev-Heisenberg model [34, 35]. We introduce the off-resonance limit of the model as well as a possibility to describe the system near resonances. In Sec. III we discuss the results for the materials  $\alpha\text{-RuCl}_3$ ,  $\alpha\text{-Li}_2\text{IrO}_3$  and  $\text{Na}_2\text{IrO}_3$ . In Sec. IIIB we study heating, and determine frequencies where Floquet driving without any considerable heating is possible. For these frequencies we then investigate the effects of Floquet driving on the Kitaev, Heisenberg and  $\Gamma$  terms in Sec. IIIC. Furthermore we also consider third-nearest-neighbor Heisenberg terms (Sec. IIID) and the impact of the polarization angle on the bond dependent Kitaev, Heisenberg and  $\Gamma$  interactions (Sec. IIIE). Section IV concludes the paper and gives a summary of the results obtained as well as an outlook to promising future studies.

## II. THEORY

### A. Effective model

The materials considered in this paper have strong Coulomb repulsion, stabilizing a  $d^5$  configuration with one hole residing on each site. Taking into account virtual excitations with two holes on one site via second order perturbation theory, gives rise to a Kugel-Khomskii-

type model [36]. Due to strong spin-orbit coupling (SOC) present in the considered materials, we can simplify the Hamiltonian further with a projection into the  $j_{\text{eff}} = 1/2$  pseudospin basis. This leads to the well-known Kitaev-Heisenberg model [37].

Coupling to a periodic light field enters via Peierls substitution into the Hubbard model

$$H_{\text{kin}}(t) = - \sum_{\substack{\gamma, \sigma \\ \langle ij \rangle_\gamma}} e^{i(\mathbf{r}_j - \mathbf{r}_i) \mathbf{A}(t)} \underbrace{\mathbf{c}_{i, \sigma}^\dagger}_{\Omega(t)} \underbrace{\mathbf{T}^\gamma \mathbf{c}_{i, \sigma}}_{\hat{v}_{ij}}, \quad (1)$$

where  $\mathbf{c}_i = (c_{i,x,\sigma}, c_{i,y,\sigma}, c_{i,z,\sigma})$  ( $\mathbf{c}_i^\dagger$ ) annihilates (creates) a hole at site  $i$  with spin  $\sigma$ . For  $d$ -orbitals, we used the notation  $yz(x)$ ,  $zx(y)$ , and  $xy(z)$  introduced in [35]. The bond-dependent hopping matrices  $\mathbf{T}^\gamma$  are given by

$$\mathbf{T}^z = \begin{pmatrix} t_1^z & t_2^z & t_4^z \\ t_2^z & t_1^z & t_4^z \\ t_4^z & t_4^z & t_3^z \end{pmatrix}, \quad \mathbf{T}^x = \begin{pmatrix} t_3^x & t_4^x & t_4^x \\ t_4^x & t_1^x & t_2^x \\ t_4^x & t_2^x & t_1^x \end{pmatrix}, \quad \mathbf{T}^y = \begin{pmatrix} t_1^y & t_4^y & t_2^y \\ t_4^y & t_3^y & t_4^y \\ t_2^y & t_4^y & t_1^y \end{pmatrix}. \quad (2)$$

Light interaction  $\Omega(t)$  depends on the vector potential  $\mathbf{A}(t)$  and the vector  $\mathbf{r}_{ij}$ , between nearest-neighbors (NN)  $i$  and  $j$ . In this paper we will primarily focus on linear polarized (LP) light, i.e. the vector potential  $\mathbf{A}(t) = (E_x, E_y) \sin(\omega t)$ . With this at hand  $\Omega(t)$  becomes  $\sum_{l=-\infty}^{\infty} \mathcal{J}_{-l}(u_{ij}) e^{-il\omega t}$ , where  $\mathcal{J}_{-l}(u_{ij})$  are Bessel functions of first kind and  $u_{ij}^\gamma = e/\omega \mathbf{r}_{ij}^\gamma E_0 (\cos(\varphi), \sin(\varphi))$ . The on site interactions can be described with a Kanamori Hamiltonian [38]

$$\begin{aligned} H_{\text{int}} = & U \sum_{i,\alpha} n_{i\alpha\uparrow} n_{i\alpha\downarrow} + U' \sum_{i,\sigma} \sum_{\alpha < \beta} n_{i\alpha\sigma} n_{i\beta-\sigma} \\ & + (U' - J_H) \sum_{i,\sigma} \sum_{\alpha < \beta} n_{i\alpha\sigma} n_{i\beta\sigma} \\ & - J_H \sum_{i,\alpha \neq \beta} (c_{i\alpha\uparrow}^\dagger c_{i\alpha\downarrow} c_{i\beta\downarrow}^\dagger c_{i\beta\uparrow} - c_{i\alpha\uparrow}^\dagger c_{i\alpha\downarrow}^\dagger c_{i\beta\downarrow} c_{i\beta\uparrow}), \quad (3) \end{aligned}$$

with intraorbital interaction  $U$ , interorbital interaction  $U' = U - 2J_H$  and Hund's coupling  $J_H$ .

Due to the time dependence in  $H_{\text{kin}}(t)$ , we apply time dependent perturbation theory. Here we limit ourselves to the subspace of states with zero and one doublon-holon (DH) pair, meaning we only consider virtual  $d^5 d^5 \rightarrow d^6 d^4 \rightarrow d^5 d^5$  excitations [32].

Writing down the time-dependent Schrödinger equations for this subspace yields

$$i\delta_t |\Psi_0\rangle_t = H_{\text{int}} |\Psi_0\rangle_t + \sum_m P_0 H_{\text{kin}}(t) |\Psi_{1,m}\rangle_t \quad (4)$$

$$i\delta_t |\Psi_{1,m}\rangle_t = P_{1,m} H_{\text{kin}}(t) |\Psi_0\rangle_t + (T_{mm} + H_{\text{int}}) |\Psi_{1,m}\rangle_t, \quad (5)$$

with  $P_0$  the projector on the zero DH pair subspace, and  $P_{1,m}$  the projector on the one-DH pair subspace with energy  $E_m$ .  $|\Psi_{1,m}\rangle$  denotes the subspace of one DH pair with energy  $E_m$ . Propagation of the doublon and holon through the lattice within the associated subspace is described by  $T_{mm} = P_{1,m} H_{\text{kin}}(t) P_{1,m}$ . We dropped  $T_{mm'}$

terms, which couple two energetically distinct subspaces with one doublon holon pair, justified by [32].

$T_{mm}$  can be averaged over time as shown in [7], which yields  $\bar{T}_{mm} = \mathcal{J}_0(u_{ij}) P_{1,m} \hat{v}_{ij} P_{1,m}$ . With this at hand we rewrite (5) to

$$|\Psi_{1,m}\rangle_t = \sum_{ij,l} \frac{1}{\Delta E_m - l\omega + \bar{T}_{mm}} e^{-il\omega t} \mathcal{J}_{-l}(u_{ij}) v_{ij}^{m,0} |\Psi_0\rangle_t, \quad (6)$$

with  $v_{ij}^{m,0} = P_{1,m} v_{ij} P_0$  and  $\Delta E_m = E_m^1 - E_0$ . Here we performed a partial integration over time and dropped terms  $\mathcal{O}(t_h/U^2)$ . Plugging (6) into (4), we derive the effective time-dependent Hamiltonian

$$H_{\text{eff}}(t) = \sum_{ij,k,l,m} v_{ij}^{0,m} \frac{\mathcal{J}_k(u_{ij}) \mathcal{J}_{-l}(u_{ij}) e^{i(k-l)\omega t}}{\Delta E_m - l\omega + \bar{T}_{mm}} v_{ij}^{m,0}. \quad (7)$$

In contrast to the time independent case the hopping amplitude is now modulated by frequency  $\omega$ , amplitude  $E_0$  and angle  $\varphi$  of the incoming light.

## B. Floquet Formalism

In Sec. II A, we derived an effective Hamiltonian periodic in time. It has been shown that Floquet theory can describe these systems with an effective time-independent Hamiltonian  $\bar{H}_{\text{eff}}$  [33, 39, 40]. For  $\omega \gg t$  a Magnus expansion up to first non-vanishing order [8] is sufficient to derive the time independent Floquet Hamiltonian

$$\bar{H}_{\text{eff}} = \sum_{ij,l,m} v_{ij}^{0,m} \frac{\mathcal{J}_l(u_{ij})^2}{\Delta E_m - l\omega + \bar{T}_{mm}} v_{ij}^{m,0}. \quad (8)$$

For  $U \gg \lambda \gg t$  the effective Floquet Hamiltonian can be projected into the  $j_{\text{eff}} = 1/2$  basis favored by SOC [34, 35]

$$\begin{aligned} \bar{H}_{\text{eff}} = & \sum_{(ij) \in \alpha\beta(\gamma)} [J^\gamma \mathbf{S}_i \mathbf{S}_j + K^\gamma S_i^\gamma S_j^\gamma + \Gamma^\gamma (S_i^\alpha S_j^\beta + S_i^\beta S_j^\alpha) \\ & + \Gamma'^\gamma (S_i^\alpha S_j^\gamma + S_i^\gamma S_j^\alpha + S_i^\beta S_j^\gamma + S_i^\gamma S_j^\beta)]. \quad (9) \end{aligned}$$

This takes the form of a Kitaev-Heisenberg model, with the difference being that the factors  $J^\gamma, K^\gamma, \Gamma^\gamma$ , and  $\Gamma'^\gamma$  depend on frequency  $\omega$ , amplitude  $E_0$  and light angle  $\varphi$  in addition to the bond direction  $\gamma$ . The interaction

terms therefore become

$$J^\gamma = \sum_{l=-\infty}^{\infty} \mathcal{J}_l^2(u_{ij}^\gamma) \frac{4}{27} \left\{ [-9(t_4^\gamma)^2 + 2(t_1^\gamma - t_3^\gamma)^2] \right. \\ \left. \times \mathcal{A}_l(\omega, U, J_H) + (2t_1^\gamma + t_3^\gamma)^2 \mathcal{B}_l(\omega, U, J_H) \right\}, \quad (10)$$

$$K^\gamma = \sum_{l=-\infty}^{\infty} \mathcal{J}_l^2(u_{ij}^\gamma) \frac{4}{9} [(t_1^\gamma - t_3^\gamma)^2 - 3((t_2^\gamma)^2 - (t_4^\gamma)^2)] \\ \times \mathcal{A}_l(\omega, U, J_H), \quad (11)$$

$$\Gamma^\gamma = \sum_{l=-\infty}^{\infty} \mathcal{J}_l^2(u_{ij}^\gamma) \frac{4}{9} [3(t_4^\gamma)^2 + 2t_2^\gamma(t_1^\gamma - t_3^\gamma)] \mathcal{A}_l(\omega, U, J_H), \quad (12)$$

$$\Gamma'^\gamma = - \sum_{n=-\infty}^{\infty} \mathcal{J}_n^2(u_{ij}^\gamma) \frac{4}{9} (t_4^\gamma(t_1^\gamma - t_3^\gamma - 3t_2^\gamma)) \mathcal{A}_l(\omega, U, J_H), \quad (13)$$

with

$$\mathcal{A}_l(\omega, U, J_H) = g_{dh}(U - 3J_H - l\omega) - g_{dh}(U - J_H - l\omega), \\ \mathcal{B}_l(\omega, U, J_H) = g_{dh}(U + 2J_H - l\omega) + 2g_{dh}(U - 3J_H - l\omega). \quad (14)$$

Notably for LP light the bond dependency additionally enters via the Bessel functions  $\mathcal{J}_l(u_{ij}^\gamma)$ . In case of circular polarized (CP) light, the bond dependence is only influenced by  $\mathbf{T}^\gamma$  and  $u_{ij}$  is bond independent [5, 31]. We will discuss advantages of both polarization types in more detail in Sec. III E.

In the pseudospin base the virtual  $d^4d^6$  excitations become  $j = 1/2, j = 1/2$  ( $d_1$ ) and  $j = 3/2, j = 1/2$  ( $d_2$ ) excitations. It has already been shown [30], that only the Heisenberg term (10) includes  $d_1$  excitations. These are described by the term  $\propto \mathcal{B}_l(\omega, U, J_H)$ . Terms  $\propto \mathcal{A}_l(\omega, U, J_H)$  in (10)-(13) describe a  $d_2$  excitation.

The Greens function  $g_{dh}$  captures the propagation of the DH pair before decaying into the  $d^5d^5$  subspace again

$$g_{dh} = \langle \Psi_0 | c_{j\beta\sigma}^\dagger c_{i\alpha\sigma} \frac{1}{\Delta E_m - l\omega + \bar{T}_{mm}} P_{1,m} c_{i\alpha\sigma}^\dagger c_{j\beta\sigma} | \Psi_0 \rangle. \quad (15)$$

Since we neglected  $T_{mm'}$ , the DH propagation takes only place in the subspace with energy  $E_m$ .

If  $|\Delta E_m - l\omega| \gg \bar{T}_{mm}$ , i.e. for off-resonant incoming light, the propagation in the one DH subspace is negligible, meaning the Green's function simply becomes  $g_{dh}(\Delta E_m - l\omega) \approx 1/(\Delta E_m - l\omega)$ . Heating effects near the resonance are neglected in this off-resonance approximation (ORA).

In case of  $\Delta E_m \approx l\omega$ , the propagation of the DH pair in the excited subspace  $T_{mm}$  is no longer negligible, and the ORA may break down. We therefore investigate the retracable path approximation (RPA) valid near resonances. The RPA [41] is a method to capture the behavior near the resonance for a one-band model. This method was already used to capture heating in multi-band spin-orbital models for  $\text{YTiO}_3$  and  $\text{LaTiO}_3$  [7, 32].

Let us first comment on the RPA's applicability. If there was only the  $j = \frac{1}{2}$  doublet, the Kitaev-Heisenberg model could be seen as a quasi one-band model. In reality, however, there is also the possibility of  $d_2$  in addition to  $d_1$  doublons, i.e., excitation of a hole into the  $j = \frac{3}{2}$  states. Additionally, the four  $j = \frac{3}{2}$  states correspond to two 'bands' already by themselves. A one-band approach can then only work as long as mixing between  $d_1$  and  $d_2$  doublons remains small and if the  $j = \frac{3}{2}$  states can be neatly separated into two weakly mixed bands. Fortunately, resonant inelastic X-ray experiments indicate that this is the case, because trigonal distortion splits the two  $j = \frac{3}{2}$  sub-bands [42-44], which suppresses their mixing. The Green's functions relating to  $d_1$  doublons and to the two sub-bands can then be approximated as independent one-band problems. Projecting (15) into the pseudospin basis leaves us then with different Green's functions, for  $d_1$  doublons with hopping amplitudes  $t_{B,1}$  and for  $d_2$  doublons with hopping amplitude  $t_{B,2}$ .

In order to perform the RPA we first rewrite the DH Green's function in terms of a holon  $g_h$  and a doublon  $g_d$  Green's function, assuming that holon and doublon movements are uncorrelated. This can be done by a convolution integral as shown in [7, 32]. Only doublon and holon paths in the excited subspace that end at their starting point are allowed. In addition, we exclude "loop" paths, leaving only retracable paths [41]. A detailed derivation can be found in [32]

For this approximation the Greens function becomes complex and no longer diverge at  $\Delta E_m = l\omega$ . Its imaginary part describes the heating due to DH propagation. The bandwidth of the heating is  $2\sqrt{z - 1}t_B$  [7], with the coordination number of the lattice  $z$  and the DH hopping strength  $t_B$ . In the remainder of the paper we set  $t_B = t_{B,1} = t_{B,2}$ .

### III. RESULTS

#### A. Materials

As promising candidates for a realization of the  $J$ - $K$ - $\Gamma$  model several iridates and ruthenates have been suggested [9, 26, 28, 30, 35, 46]. In this paper we will focus on the three compounds  $\text{Na}_2\text{IrO}_3$ ,  $\alpha\text{-Li}_2\text{IrO}_3$ , and  $\alpha\text{-RuCl}_3$ . In the following discussion we use the hopping parameters of [30] with the only distinction that we chose symmetrized hopping parameters  $t_1^{x/y} = (t'_{1a} + t'_{1b})/2$  and  $t_4^{x/y} = (t'_{4a} + t'_{4b})/2$ . The values of Hund's coupling  $J_H$  and Coulomb repulsion  $U$  for iridates and ruthenates are taken from [45] and [28] respectively. All considered parameters are listed in Tab. I.

Notably all materials possess an anisotropy in  $z$ -direction, which intrinsically calls for bond dependent treatment of  $J, K$ , and  $\Gamma$ .

Material	Na <sub>2</sub> IrO <sub>3</sub>		α-Li <sub>2</sub> IrO <sub>3</sub>		α-RuCl <sub>3</sub>	
$U$	1.7		1.7		3.0	
$J_H$	0.3		0.3		0.5	
NN	1 <sup>st</sup>	3 <sup>rd</sup>	1 <sup>st</sup>	3 <sup>rd</sup>	1 <sup>st</sup>	3 <sup>rd</sup>
$t_1^z$	33.1	-9.3	55.0	-6.4	50.9	-8.2
$t_2^z$	264.3	-13.8	219.0	-13.5	158.2	-7.4
$t_3^z$	26.6	-36.8	-175.1	-33.3	-154.0	-39.5
$t_4^z$	-11.8	16.6	-124.5	16.6	-20.2	11.7
$t_1^{x/y}$	38.8	-8.4	76.3	-6.3	45.4	-7.7
$t_2^{x/y}$	269.3	-12.7	252.7	-13.4	162.2	-7.8
$t_3^{x/y}$	-19.4	-35.3	-108.8	-33.0	-103.1	-41.4
$t_4^{x/y}$	-23.4	16.0	-9.3	15.8	-13.0	11.7

TABLE I. Parameters for Na<sub>2</sub>IrO<sub>3</sub>, α-Li<sub>2</sub>IrO<sub>3</sub>, and α-RuCl<sub>3</sub>. 1<sup>st</sup>- and 3<sup>rd</sup>-nearest-neighbor (NN) hopping parameters in meV are taken from [30]. Coulomb repulsion  $U$  and Hund's coupling in eV taken from [45] for iridates and from [28] for ruthenates

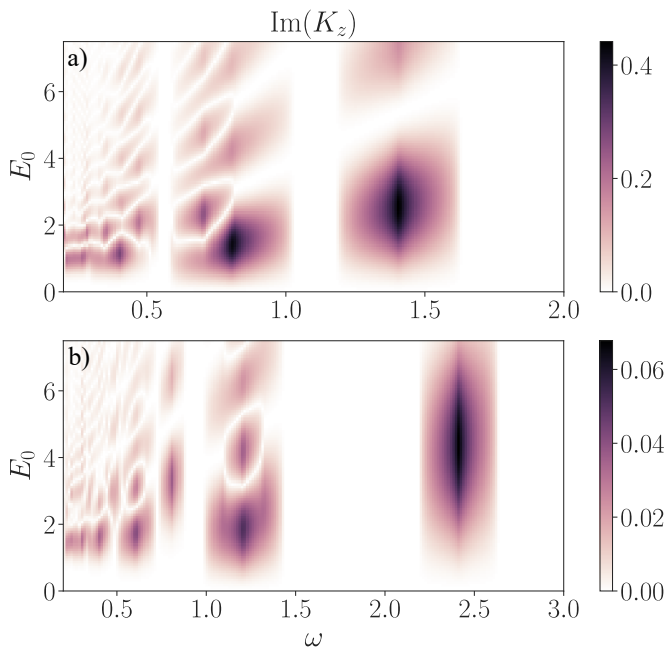


FIG. 1. Imaginary part of  $K_z$  plotted for varying light frequency  $\omega$  and amplitude  $E_0$  in eV, with the parameter set of Na<sub>2</sub>IrO<sub>3</sub> a) and α-RuCl<sub>3</sub> b). For the calculations of the Green's functions the retracable path approximation (RPA) was used.

### B. Heating in dependency of $\omega$ and $E_0$

In this section we investigate possible heating effects arising from DH propagation captured by the RPA. The bandwidth  $t_B$  is set to  $t_B = 0.04$  eV. Representative for the other interactions, Kitaev interactions are analyzed in dependency of the frequency  $\omega$  and the amplitude  $E_0$  of the LP light. We only discuss z-Bond terms to get an qualitative understanding of heating effects. To do so we examine the imaginary part of the Kitaev interaction  $K_z$  (11) calculated with RPA.

For Na<sub>2</sub>IrO<sub>3</sub> [Fig. 1(b)] heating is present around a relatively broad area around the resonances, leaving a narrow area around  $\omega = 1.1$  eV, where heating-free driving is possible. In this area, from now on referred to as driving corridor the ORA is expected to be valid. For frequencies  $\omega < U - 3J_H$  driving without heating becomes difficult due to a multitude of resonances. Evidently the width of the driving corridor is not only dependent on  $t_B$  but also the magnitude of  $J_H$ . Increasing  $J_H$  separates the resonances and therefore enhances the driving corridor. A broad driving corridor is a desirable feature for experiments. In Li<sub>2</sub>IrO<sub>3</sub> heating effects are very similar to Na<sub>2</sub>IrO<sub>3</sub>. Therefore we omit a more detailed discussion in this section.

In comparison to iridates, α-RuCl<sub>3</sub> has significant larger Coulomb repulsion and Hund's interaction. Fig. 1(b) clearly displays that the resonance peaks are further apart than in Fig. 1(a), causing a broader driving corridor. This makes α-RuCl<sub>3</sub> a more promising candidate for Floquet engineering than iridate compounds. Also the ORA appears to be well justified within the driving corridor.

We conclude that both iridates and ruthenates are susceptible to Floquet engineering within a certain driving corridor. This driving corridor is mainly determined by  $J_H$  and  $t_B$ . Materials with large Hund's interaction and small  $t_B$  should be primed for Floquet engineering. Within this driving corridor the ORA is expected to be valid and differences to the RPA should be minute.

### C. Floquet engineering in the ORA

After considering possible influences of heating, we focus on Floquet driving within the driving corridor between the resonances at  $U - 3J_h$  and  $U - J_H$ . To do so we set the frequency to  $\omega = 1.1$  eV for iridates and  $\omega = 1.6$  eV for the ruthenate. As we can see in Fig. 2, varying  $E_0$  can change both magnitude and sign of the interaction terms. In addition to ORA results (solid lines), the results for the RPA with  $t_B = 0.4$  are displayed (dashed lines). Since the differences are minor and heating is negligible (see Sec. III B), we will from here on only discuss the ORA results.

The interaction terms for Na<sub>2</sub>IrO<sub>3</sub> are shown in Fig. 2(a). The Kitaev interaction is dominant throughout the whole parameter range, while the other terms are considerably smaller. We also note that the absolute magnitude of the interactions decreases with increasing  $E_0$ . The inset in Fig. 2(a) clearly displays that  $J$  can be tuned relative to the  $K$ ,  $\Gamma$  and  $\Gamma'$  interactions, by changing  $E_0$ .

On the z-bond of Na<sub>2</sub>IrO<sub>3</sub> this effect is particularly visible since the factor  $2t_1 + t_3$  in  $\mathcal{B}_l(\omega, U, J_H)$  becomes relatively large, due to  $t_1 > 0$  and  $t_3 > 0$ . This effect has already been discussed in [31]. However this has been done with a change of sign in  $t_3$  for α-RuCl<sub>3</sub>. It is encouraging that this effect also arises for realistic pa-

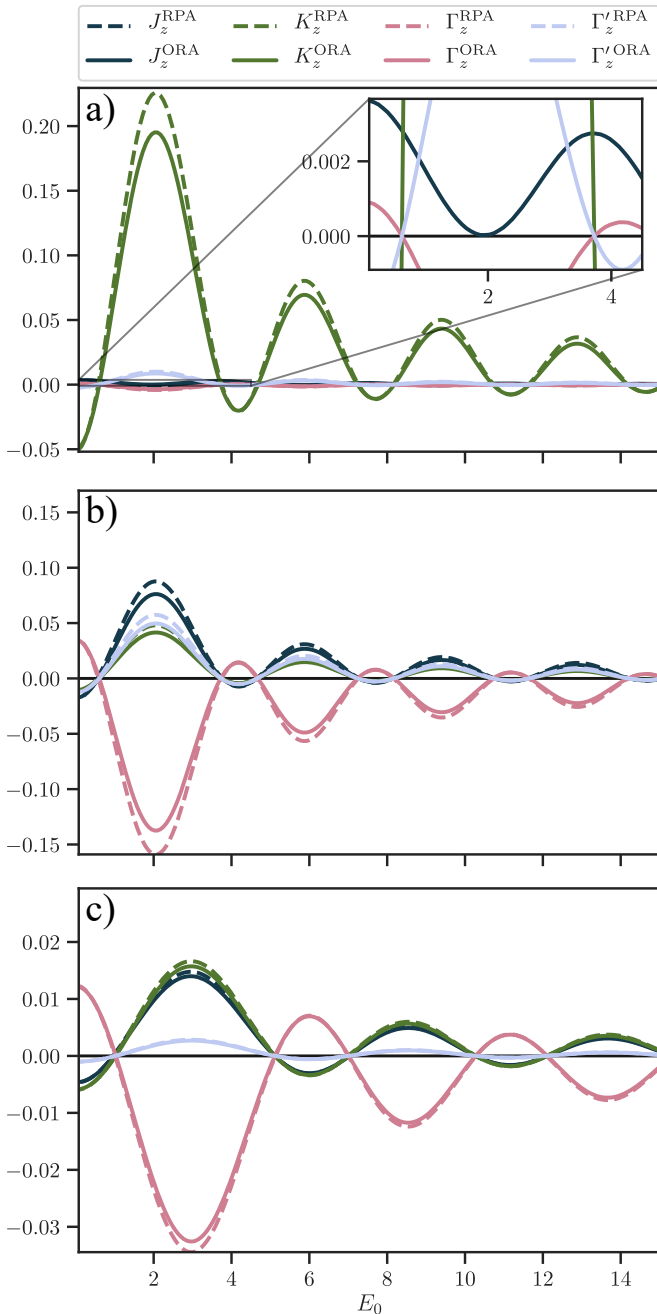


FIG. 2.  $J$ ,  $K$ ,  $\Gamma$ , and  $\Gamma'$  terms in dependency of the light amplitude  $E_0$  in eV for  $\text{Na}_2\text{IrO}_3$  parameter set with fixed frequency  $\omega = 1.1$  eV a).  $\alpha\text{-Li}_2\text{IrO}_3$  with  $\omega = 1.1$  eV, and  $\alpha\text{-RuCl}_3$  with  $\omega = 1.6$  eV are displayed in b) and c) respectively. The real part of the RPA is displayed with dashed lines, the ORA with solid lines. The inset in a) shows a zoom in for  $0 < E_0 < 5$ .

rameters in  $\text{Na}_2\text{IrO}_3$ . For a tuning of  $J$  it is sufficient to have a comparable energy scale of  $\mathcal{A}_l(\omega, U, J_H)$  and  $\mathcal{B}_l(\omega, U, J_H)$ . On the  $z$ -Bond of  $\text{Na}_2\text{IrO}_3$ , we therefore have the ability to completely turn off the Heisenberg interactions at  $E_0 \approx 2$  eV and reduce the model to a  $K$ - $\Gamma$ -model. However this is not the case for the  $x$ - and  $y$ -

Bond in  $\text{Na}_2\text{IrO}_3$ , due to the fact that  $t_3^{x/y} < 0$  for these bonds, which reduces the influence of  $\mathcal{B}_l(\omega, U, J_H)$ .

In  $\text{Li}_2\text{IrO}_3$  the Kitaev interaction is far less dominant, and the  $J$ ,  $\Gamma$ ,  $\Gamma'$  terms all are significant [Fig. 2(b)]. Moreover, the values of  $t_1$  and  $t_3$  (see Tab.I) imply a low tunability of  $J$ . In Fig. 2(b) we indeed see that the  $J$  term is almost in phase with the other terms. It is however still possible to adjust magnitude and sign of the interaction terms with the help of light frequency and amplitude.

For  $\alpha\text{-RuCl}_3$  results for all interaction parameters are shown in Fig. 2(c). As in the case of  $\alpha\text{-Li}_2\text{RuO}_3$ , the  $J$  parameter is mostly in phase with the other terms. Again the reason for that is the sub-optimal combination of the  $t_1$  and  $t_3$  parameters. Compared to iridates, the frequency of the oscillation is significantly lower. The origin is the larger  $\omega$  needed to suppress heating in ruthenates, which enters the Bessel function as  $\frac{1}{\omega}$ .

The results of Fig. 2(c) thus confirm [31], in that for realistic parameters and only considering NN interactions a tuning of  $J$ ,  $K$ ,  $\Gamma$ , and  $\Gamma'$  relative to each other is not possible. However we found that in other materials like  $\text{Na}_2\text{IrO}_3$  a tuning of the Heisenberg term is possible due to a more suitable combination of the hopping parameters.

#### D. Third-nearest-neighbor Heisenberg interactions

Third-nearest-neighbor ( $3^{\text{rd}}$  NN) Heisenberg interactions are argued to have a significant impact on the formation of the zig-zag ground state found in iridates and ruthenates [47]. Especially in  $\text{Na}_2\text{IrO}_3$ ,  $J_3$  is a main reason for the absence of the KSL [30]. For this reason, we investigate the possibility of tuning  $J_3(E_0, \omega)$  relative to the NN interactions.

$J_3$  is calculated in the same manner as  $J$  [with (10)]. The hopping parameters considered for  $J_3$  are taken from [30] and listed in Tab. I. We note that the requirement for a significant tuning, a large  $|(2t_1 + t_3)|$ , is fulfilled for all materials. In addition, the larger distance  $|r_{ij}|$  for third nearest neighbors changes the frequency of  $\mathcal{J}_{-l}(u_{ij})$ . Together with the promising hopping parameters, this suggests that  $J_3$  can be tuned relative to the other interaction parameters, similar to  $J_z$  in  $\text{Na}_2\text{IrO}_3$ .

Since we want to compare interaction terms of bonds with different directions ( $3^{\text{rd}}$  NN and NN) CP light is more suitable. This is the case since for CP  $u_{ij}^c = e/\omega E_0 |\mathbf{r}_{ij}^c|$  becomes bond independent, due to  $|\mathbf{r}_{ij}^c| = |r_{ij}|$  for NN's. The only distinctions between NN and  $3^{\text{rd}}$  NN are therefore the distance  $|r_{ij}|$  and the hopping parameters.

In Fig. 3 the normalized  $\bar{K}$ ,  $\bar{\Gamma}$ ,  $\bar{\Gamma}'$  and  $\bar{J}_3$  interactions are shown. As normalization factor the maximum of the respective interaction in the considered  $E_0$  range is chosen. It becomes obvious that for all materials  $J^3$  decreases significantly faster with  $E_0$  than the NN interactions. This gives a pathway to suppress  $J^3$  via the light

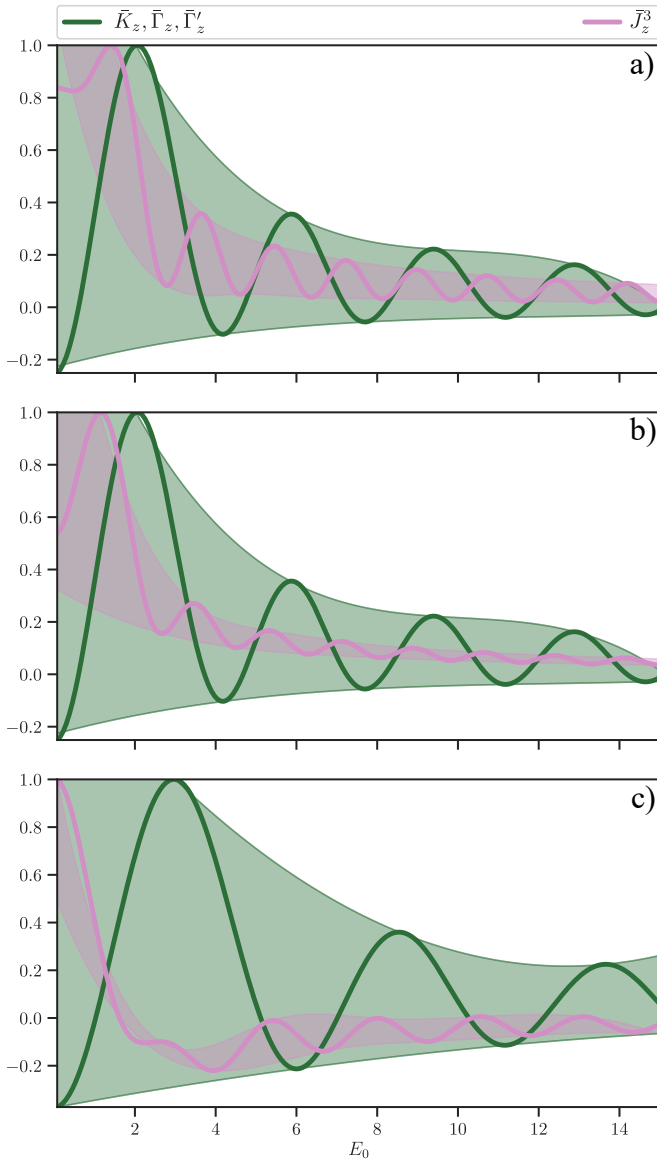


FIG. 3. Comparison of normalized  $\bar{K}_z, \bar{\Gamma}_z, \bar{\Gamma}'_z$  and third-nearest-neighbor Heisenberg  $\bar{J}_z^3$  interactions in dependency of  $E_0$  in eV. For  $\text{Na}_2\text{IrO}_3$  a) and  $\alpha\text{-Li}_2\text{IrO}_3$  b) the frequency is set to  $\omega = 1.1$  eV. For  $\alpha\text{RuCl}_3$  c) the frequency is  $\omega = 1.6$  eV.

amplitude  $E_0$ . Due to the differing frequencies for NN and 3<sup>rd</sup> NN it is also possible to completely turn off  $J^3$  while having finite NN interactions.

In general CP light is well suited for isotropic materials since it does not change the magnitude of bond interactions relative to each other. However if a material has anisotropic interaction terms, LP light has significant advantages over CP light, which we discuss in the following section.

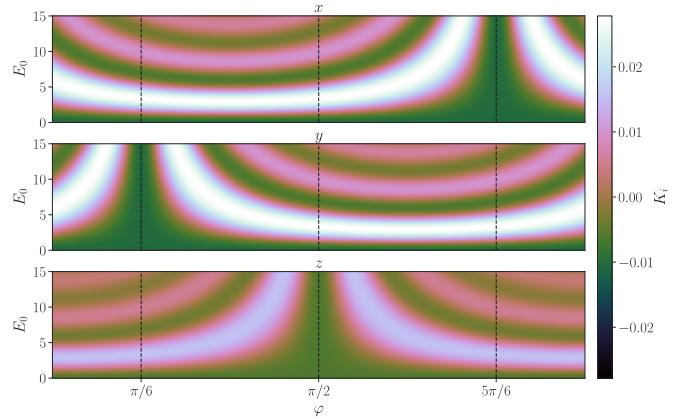


FIG. 4. The magnitude of the Kitaev interaction term for  $x$ -,  $y$ - and  $z$ -bond depending on the light angle  $\varphi$  and the light amplitude  $E_0$  in eV is shown for  $\alpha\text{-RuCl}_3$ .

### E. Light Angle

Up until now we only considered LP light parallel to the  $z$ -axis. In general LP light can point in an arbitrary direction, making it a parameter that is experimentally adjustable. The angle of the incoming light has an impact on the interaction terms, therefore it should be possible to tune the interactions by just changing the light angle  $\varphi$ . We expect the light angle  $\varphi$  to alter the relative strengths of the  $x$ ,  $y$  and  $z$  interaction terms, hence we now consider the  $x$  and  $y$  bond in addition to the  $z$  bond.

The focus in this chapter is tuning the Kitaev interactions, which is why for the remainder of the section we only consider  $K_x, K_y$ , and  $K_z$ . We calculate the Kitaev interactions depending on the light angle  $\varphi$  and the driving amplitude  $E_0$  with the ORA. Since the interaction terms are  $\pi$ -periodic we only consider  $\varphi \in [0, \pi]$ . The results for  $\alpha\text{-RuCl}_3$  at  $\omega = 1.6$  eV are displayed in Fig. 4.

The corridors at  $\varphi = \pi/6, \pi/2$ , and  $5\pi/6$  for the  $y$ -,  $z$ - and  $x$ -bond interaction respectively are the most notable features. For these angles the Kitaev term of the respective bond is independent of  $E_0$ . We can see that if  $\mathbf{r}_{ij} \perp \mathbf{A}(t)$  the interaction decouples from the light, since  $u_{ij} = 0$ . Therefore it is possible to tune two bond interactions while the coupling along the remaining bond direction remains unchanged. This opens the path to eliminate anisotropies intrinsic to, e.g.,  $\alpha\text{-Li}_2\text{IrO}_3$  and  $\alpha\text{-RuCl}_3$ .

The second effect we observe is that depending on the light angle and the driving amplitude, the Kitaev interactions can have different signs for different bonds. Additionally, the magnitude of the interactions also drastically depends on the light angle  $\varphi$ . As a consequence of these two effects, the Kitaev interactions might no longer support a gapless Kitaev phase, but rather give rise to a gapped Kitaev phase, due to the strong anisotropies.

We are aware that in all considered materials the Kitaev phase is not yet realized. In this section we therefore want to discuss the nature of the Kitaev phase if it were

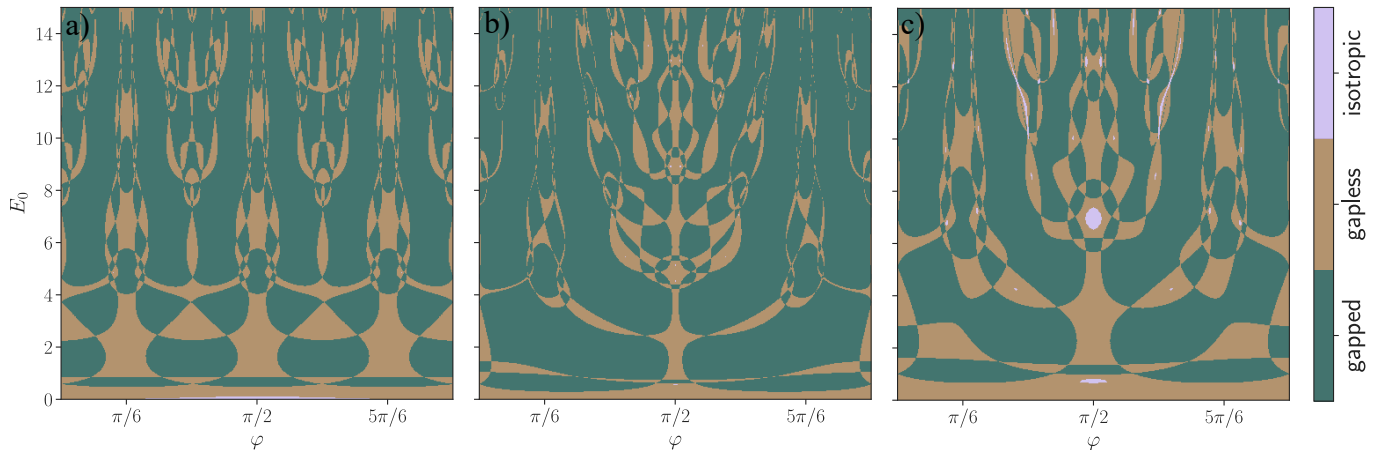


FIG. 5.  $E_0$ - $\varphi$  phase diagram where Kitaev interactions of Fig. 4 would give rise to a gapped (light blue), gapless (purple) and isotropic (orange) Kitaev phase. The terms gapless and isotropic are defined by the criteria in the text. Calculations were done for  $\text{Na}_2\text{IrO}_3$  a),  $\alpha\text{-Li}_2\text{IrO}_3$  b), and  $\alpha\text{-RuCl}_3$  c).

to be realized. Interactions giving rise to a gapped (gapless) Kitaev phase are referred to as gapped (gapless) interactions.

The criterion for gapless interactions  $K_\alpha + K_\beta > K_\gamma$ , with  $\alpha, \beta, \gamma \in (x, y, z)$ , does not hold for arbitrary  $\varphi$  and  $E_0$ . Applying this condition to the Kitaev terms of Fig. 4, we see where gapped and gapless interactions arise. The results for the different materials are displayed in Fig. 5. We also added isotropic interactions with the condition  $|K_\alpha - K_\beta| < \epsilon$ , for all combinations of  $\alpha, \gamma$  and  $\epsilon = 10^{-3}$ . This isotropic interaction is included to highlight that Floquet engineering is capable of increasing the isotropy in materials [Fig. 5(c)].

For  $\text{Na}_2\text{IrO}_3$  we observe that without driving the NN Kitaev interactions are already almost isotropic. Turning on the LP light then breaks the isotropy and also gives rise to gapped interactions. Around  $\varphi = \pi/6, \pi/2$ , and  $5\pi/6$  the interactions are very likely to be gapless.

In case of  $\alpha\text{-Li}_2\text{RuO}_3$  the system has gapless interactions in the absence of LP light. Again turning on LP light can lead gapped interactions. In contrast to  $\text{Na}_2\text{IrO}_3$ , there is only a preference of gapless interactions at  $\pi/2$ . This can be explained due to the large intrinsic anisotropy in  $z$ -direction. Also the areas of a gapped interactions are significantly larger than in  $\text{Na}_2\text{IrO}_3$  leading to the conclusion that deriving a gapless interaction in the presence of a LP light field might be complicated.

Like in  $\alpha\text{-Li}_2\text{RuO}_3$ , the high intrinsic anisotropy in  $\alpha\text{-RuCl}_3$  allows a stable gapless interaction only at  $\pi/2$ . However unlike the case in the iridate, the ruthenate actually can be driven into a isotropic interaction at  $\varphi \approx \pi/2$  and  $E_0 \approx 7$  eV.

#### IV. DISCUSSION AND CONCLUSIONS

We have investigated Floquet engineering for a variety of candidate Kitaev materials. To do so we derived an

effective Floquet Kitaev-Heisenberg model for LP light similar to the CP light model of [35]. The Green's functions in (15) were approximated with the ORA and RPA.

With help of the RPA we were able to determine a frequency range where the ORA is valid. In addition, we also identified frequencies where heating can be assumed to be negligible. This lead us to the conclusion that Floquet engineering in ruthenates should in principle be more promising than in iridates.

For suitable off-resonance frequencies, we investigated the influence of the light amplitude on the nearest-neighbor interaction terms (Fig. 2), where our results qualitatively agree with the results reported in Ref. [31]. We thus observe that tuning in magnitude and sign of the interactions in dependency of the light amplitude is possible. For instance, Heisenberg  $J$  can be tuned relative to the other parameters, especially on the  $z$ -bond of the  $\text{Na}_2\text{IrO}_3$  compound.

Going beyond nearest-neighbors, we find that third-nearest-neighbor Heisenberg interactions  $J_3$  [30] are quite susceptible to Floquet tuning. With the right setting of frequency and amplitude, a significant decrease of the third-nearest-neighbor interaction terms should be achievable in all considered materials. Circular polarized is expected to work better than linear polarization, and could be used to suppressing zig-zag order, which is stabilized by  $J_3$  and competes with the Kitaev spin liquid.

Linear polarized light, on the other hand, allows us to tune the interactions in different directions, with the help of the angle of the incoming light. Starting from a pure Kitaev model, this can either lead to a gapped model or more isotropic Kitaev interactions. It is also possible to decouple single bonds completely from the light so that they remain unaffected, so one can specifically "erase" anisotropies in one direction.

After investigating the more traditional Kitaev candidate materials, it would be interesting to consider materials which at first glance seem unattractive due to e.g.

high anisotropies, which could be tuned into promising candidates with the help of Floquet engineering. Finally, materials with strong  $U$  and  $J_H$  are particularly promis-

ing, due to a wide driving corridor. This suggests materials based on  $3d$  elements [48, 49], where these interactions tend to be stronger.

- 
- [1] A. Eckardt, Colloquium: Atomic quantum gases in periodically driven optical lattices, *Rev. Mod. Phys.* **89**, 011004 (2017).
- [2] T. Oka and S. Kitamura, Floquet Engineering of Quantum Materials, *Annual Review of Condensed Matter Physics* **10**, 387 (2019).
- [3] J. H. Mentink, Manipulating magnetism by ultrafast control of the exchange interaction, *Journal of Physics: Condensed Matter* **29**, 453001 (2017).
- [4] J. Mentink, K. Balzer, and M. Eckstein, Ultrafast and reversible control of the exchange interaction in Mott insulators, *Nature Communications* **6** (2015).
- [5] M. Claassen, H.-C. Jiang, B. Moritz, and T. P. Devereaux, Dynamical time-reversal symmetry breaking and photo-induced chiral spin liquids in frustrated Mott insulators, *Nature Communications* **8** (2017).
- [6] M. Bukov, M. Kolodrubetz, and A. Polkovnikov, Schrieffer-Wolff Transformation for Periodically Driven Systems: Strongly Correlated Systems with Artificial Gauge Fields, *Phys. Rev. Lett.* **116**, 125301 (2016).
- [7] J. Liu, K. Hejazi, and L. Balents, Floquet Engineering of Multiorbital Mott Insulators: Applications to Orthorhombic Titanates, *Phys. Rev. Lett.* **121**, 107201 (2018).
- [8] T. Kuwahara, T. Mori, and K. Saito, Floquet-Magnus theory and generic transient dynamics in periodically driven many-body quantum systems, *Annals of Physics* **367**, 96 (2016).
- [9] S. M. Winter, A. A. Tsirlin, M. Daghofer, J. van den Brink, Y. Singh, P. Gegenwart, and R. Valentí, Models and materials for generalized Kitaev magnetism, *Journal of Physics: Condensed Matter* **29**, 493002 (2017).
- [10] X. Liu, T. Berlijn, W.-G. Yin, W. Ku, A. Tsvelik, Y.-J. Kim, H. Gretarsson, Y. Singh, P. Gegenwart, and J. P. Hill, Long-range magnetic ordering in  $\text{Na}_2\text{IrO}_3$ , *Phys. Rev. B* **83**, 220403 (2011).
- [11] F. Ye, S. Chi, H. Cao, B. C. Chakoumakos, J. A. Fernandez-Baca, R. Custelcean, T. F. Qi, O. B. Korneta, and G. Cao, Direct evidence of a zigzag spin-chain structure in the honeycomb lattice: A neutron and x-ray diffraction investigation of single-crystal  $\text{Na}_2\text{IrO}_3$ , *Phys. Rev. B* **85**, 180403 (2012).
- [12] S. K. Choi, R. Coldea, A. N. Kolmogorov, T. Lancaster, I. I. Mazin, S. J. Blundell, P. G. Radaelli, Y. Singh, P. Gegenwart, K. R. Choi, S.-W. Cheong, P. J. Baker, C. Stock, and J. Taylor, Spin Waves and Revised Crystal Structure of Honeycomb Iridate  $\text{Na}_2\text{IrO}_3$ , *Phys. Rev. Lett.* **108**, 127204 (2012).
- [13] R. D. Johnson, S. C. Williams, A. A. Haghighirad, J. Singleton, V. Zapf, P. Manuel, I. I. Mazin, Y. Li, H. O. Jeschke, R. Valentí, and R. Coldea, Monoclinic crystal structure of  $\alpha\text{-RuCl}_3$  and the zigzag antiferromagnetic ground state, *Phys. Rev. B* **92**, 235119 (2015).
- [14] Y. Cui, J. Zheng, K. Ran, J. Wen, Z.-X. Liu, B. Liu, W. Guo, and W. Yu, High-pressure magnetization and NMR studies of  $\alpha\text{-RuCl}_3$ , *Phys. Rev. B* **96**, 205147 (2017).
- [15] Z. Wang, J. Guo, F. F. Tafti, A. Hegg, S. Sen, V. A. Sidorov, L. Wang, S. Cai, W. Yi, Y. Zhou, H. Wang, S. Zhang, K. Yang, A. Li, X. Li, Y. Li, J. Liu, Y. Shi, W. Ku, Q. Wu, R. J. Cava, and L. Sun, Pressure-induced melting of magnetic order and emergence of a new quantum state in  $\alpha\text{-RuCl}_3$ , *Phys. Rev. B* **97**, 245149 (2018).
- [16] D. A. S. Kaib, S. Biswas, K. Riedl, S. M. Winter, and R. Valentí, Magnetoelastic coupling and effects of uniaxial strain in  $\alpha\text{-RuCl}_3$  from first principles, *Phys. Rev. B* **103**, L140402 (2021).
- [17] I. A. Leahy, C. A. Pocs, P. E. Siegfried, D. Graf, S.-H. Do, K.-Y. Choi, B. Normand, and M. Lee, Anomalous Thermal Conductivity and Magnetic Torque Response in the Honeycomb Magnet  $\alpha\text{-RuCl}_3$ , *Phys. Rev. Lett.* **118**, 187203 (2017).
- [18] S.-H. Baek, S.-H. Do, K.-Y. Choi, Y. S. Kwon, A. U. B. Wolter, S. Nishimoto, J. van den Brink, and B. Büchner, Evidence for a Field-Induced Quantum Spin Liquid in  $\alpha\text{-RuCl}_3$ , *Phys. Rev. Lett.* **119**, 037201 (2017).
- [19] J. A. Sears, Y. Zhao, Z. Xu, J. W. Lynn, and Y.-J. Kim, Phase diagram of  $\alpha\text{-RuCl}_3$  in an in-plane magnetic field, *Phys. Rev. B* **95**, 180411 (2017).
- [20] J. Zheng, K. Ran, T. Li, J. Wang, P. Wang, B. Liu, Z.-X. Liu, B. Normand, J. Wen, and W. Yu, Gapless Spin Excitations in the Field-Induced Quantum Spin Liquid Phase of  $\alpha\text{-RuCl}_3$ , *Phys. Rev. Lett.* **119**, 227208 (2017).
- [21] R. Henrich, A. U. B. Wolter, X. Zotos, W. Brenig, D. Nowak, A. Isaeva, T. Doert, A. Banerjee, P. Lampen-Kelley, D. G. Mandrus, S. E. Nagler, J. Sears, Y.-J. Kim, B. Büchner, and C. Hess, Unusual Phonon Heat Transport in  $\alpha\text{-RuCl}_3$ : Strong Spin-Phonon Scattering and Field-Induced Spin Gap, *Phys. Rev. Lett.* **120**, 117204 (2018).
- [22] S. Biswas, Y. Li, S. M. Winter, J. Knolle, and R. Valentí, Electronic Properties of  $\alpha\text{-RuCl}_3$  in Proximity to Graphene, *Phys. Rev. Lett.* **123**, 237201 (2019).
- [23] A. Koitzsch, C. Habenicht, E. Müller, M. Knupfer, B. Büchner, S. Kretschmer, M. Richter, J. van den Brink, F. Börrnert, D. Nowak, A. Isaeva, and T. Doert, Nearest-neighbor Kitaev exchange blocked by charge order in electron-doped  $\alpha\text{-RuCl}_3$ , *Phys. Rev. Materials* **1**, 052001 (2017).
- [24] G. Bastien, M. Roslova, M. H. Haghighi, K. Mehlawat, J. Hunger, A. Isaeva, T. Doert, M. Vojta, B. Büchner, and A. U. B. Wolter, Spin-glass state and reversed magnetic anisotropy induced by Cr doping in the Kitaev magnet  $\alpha\text{-RuCl}_3$ , *Phys. Rev. B* **99**, 214410 (2019).
- [25] S.-H. Baek, H. W. Yeo, S.-H. Do, K.-Y. Choi, L. Janssen, M. Vojta, and B. Büchner, Observation of a random singlet state in a diluted Kitaev honeycomb material, *Phys. Rev. B* **102**, 094407 (2020).
- [26] K. Foyevtsova, H. O. Jeschke, I. I. Mazin, D. I. Khomskii, and R. Valentí, Ab initio analysis of the tight-binding parameters and magnetic interactions in  $\text{Na}_2\text{IrO}_3$ , *Phys. Rev. B* **88**, 035107 (2013).

- [27] A. Biffin, R. D. Johnson, I. Kimchi, R. Morris, A. Bombardi, J. G. Analytis, A. Vishwanath, and R. Coldea, Noncoplanar and Counterrotating Incommensurate Magnetic Order Stabilized by Kitaev Interactions in  $\gamma$ - $\text{Li}_2\text{IrO}_3$ , *Phys. Rev. Lett.* **113**, 197201 (2014).
- [28] H.-S. Kim, V. S. V., A. Catuneanu, and H.-Y. Kee, Kitaev magnetism in honeycomb  $\text{RuCl}_3$  with intermediate spin-orbit coupling, *Phys. Rev. B* **91**, 241110 (2015).
- [29] A. Biffin, R. D. Johnson, S. Choi, F. Freund, S. Manni, A. Bombardi, P. Manuel, P. Gegenwart, and R. Coldea, Unconventional magnetic order on the hyperhoneycomb Kitaev lattice in  $\beta$ - $\text{Li}_2\text{IrO}_3$ : Full solution via magnetic resonant x-ray diffraction, *Phys. Rev. B* **90**, 205116 (2014).
- [30] S. M. Winter, Y. Li, H. O. Jeschke, and R. Valenti, Challenges in design of Kitaev materials: Magnetic interactions from competing energy scales, *Phys. Rev. B* **93**, 214431 (2016).
- [31] N. Arakawa and K. Yonemitsu, Floquet engineering of Mott insulators with strong spin-orbit coupling, *Phys. Rev. B* **103**, L100408 (2021).
- [32] K. Hejazi, J. Liu, and L. Balents, Floquet spin and spin-orbital Hamiltonians and doublon-holon generations in periodically driven Mott insulators, *Phys. Rev. B* **99**, 205111 (2019).
- [33] J. H. Shirley, Solution of the Schrödinger Equation with a Hamiltonian Periodic in Time, *Phys. Rev.* **138**, B979 (1965).
- [34] G. Jackeli and G. Khaliullin, Mott Insulators in the Strong Spin-Orbit Coupling Limit: From Heisenberg to a Quantum Compass and Kitaev Models, *Phys. Rev. Lett.* **102**, 017205 (2009).
- [35] J. G. Rau, E. K.-H. Lee, and H.-Y. Kee, Generic Spin Model for the Honeycomb Iridates beyond the Kitaev Limit, *Phys. Rev. Lett.* **112**, 077204 (2014).
- [36] K. I. Kugel and D. I. Khomskii, The Jahn-Teller effect and magnetism: transition metal compounds, *Soviet Physics Uspekhi* **25**, 231 (1982).
- [37] J. Chaloupka, G. Jackeli, and G. Khaliullin, Kitaev-Heisenberg Model on a Honeycomb Lattice: Possible Exotic Phases in Iridium Oxides  $\text{A}_2\text{IrO}_3$ , *Phys. Rev. Lett.* **105**, 027204 (2010).
- [38] J. Kanamori, Electron Correlation and Ferromagnetism of Transition Metals, *Progress of Theoretical Physics* **30**, 275 (1963).
- [39] H. Sambe, Steady States and Quasienergies of a Quantum-Mechanical System in an Oscillating Field, *Phys. Rev. A* **7**, 2203 (1973).
- [40] M. Bukov, L. D'Alessio, and A. Polkovnikov, Universal high-frequency behavior of periodically driven systems: from dynamical stabilization to Floquet engineering, *Advances in Physics* **64**, 139 (2015).
- [41] W. F. Brinkman and T. M. Rice, Single-Particle Excitations in Magnetic Insulators, *Phys. Rev. B* **2**, 1324 (1970).
- [42] H. Gretarsson, J. P. Clancy, X. Liu, J. P. Hill, E. Bozin, Y. Singh, S. Manni, P. Gegenwart, J. Kim, A. H. Said, D. Casa, T. Gog, M. H. Upton, H.-S. Kim, J. Yu, V. M. Katukuri, L. Hozoi, J. van den Brink, and Y.-J. Kim, Crystal-Field Splitting and Correlation Effect on the Electronic Structure of  $\text{A}_2\text{IrO}_3$ , *Phys. Rev. Lett.* **110**, 076402 (2013).
- [43] B. W. Lebert, S. Kim, V. Bisogni, I. Jarrige, A. M. Barbour, and Y.-J. Kim, Resonant inelastic x-ray scattering study of  $\alpha$ - $\text{RuCl}_3$ : a progress report, *Journal of Physics: Condensed Matter* **32**, 144001 (2020).
- [44] R. Yadav, N. A. Bogdanov, V. M. Katukuri, S. Nishimoto, J. van den Brink, and L. Hozoi, Kitaev exchange and field-induced quantum spin-liquid states in honeycomb  $\alpha$ - $\text{RuCl}_3$ , *Scientific Reports* **6** (2016).
- [45] Y. Yamaji, Y. Nomura, M. Kurita, R. Arita, and M. Imada, First-Principles Study of the Honeycomb-Lattice Iridates  $\text{Na}_2\text{IrO}_3$  in the Presence of Strong Spin-Orbit Interaction and Electron Correlations, *Phys. Rev. Lett.* **113**, 107201 (2014).
- [46] I. I. Mazin, H. O. Jeschke, K. Foyevtsova, R. Valentí, and D. I. Khomskii,  $\text{Na}_2\text{IrO}_3$  as a Molecular Orbital Crystal, *Phys. Rev. Lett.* **109**, 197201 (2012).
- [47] L. Janssen, E. C. Andrade, and M. Vojta, Magnetization processes of zigzag states on the honeycomb lattice: Identifying spin models for  $\alpha$ - $\text{RuCl}_3$  and  $\text{Na}_2\text{IrO}_3$ , *Phys. Rev. B* **96**, 064430 (2017).
- [48] H. Liu, J. Chaloupka, and G. Khaliullin, Kitaev Spin Liquid in  $3d$  Transition Metal Compounds, *Phys. Rev. Lett.* **125**, 047201 (2020).
- [49] M. Songvilay, J. Robert, S. Petit, J. A. Rodriguez-Rivera, W. D. Ratcliff, F. Damay, V. Balédent, M. Jiménez-Ruiz, P. Lejay, E. Pachoud, A. Hadj-Azzem, V. Simonet, and C. Stock, Kitaev interactions in the Co honeycomb antiferromagnets  $\text{Na}_3\text{Co}_2\text{SbO}_6$  and  $\text{Na}_2\text{Co}_2\text{TeO}_6$ , *Phys. Rev. B* **102**, 224429 (2020).